

Correlation of histopathology with magnetic resonance imaging in Kienbock disease.

著者別名	小川 健, 西浦 康正, 原 友紀, 岡本 嘉一, 落合 直之
journal or publication title	The journal of hand surgery
volume	37
number	1
page range	83-89
year	2012-01
権利	(C) 2012 American Society for Surgery of the Hand. Published by Elsevier Inc. NOTICE: this is the author's version of a work that was accepted for publication in The journal of hand surgery. Changes resulting from the publishing process, such as peer review, editing, corrections, structural formatting, and other quality control mechanisms may not be reflected in this document. Changes may have been made to this work since it was submitted for publication. A definitive version was subsequently published in PUBLICATION, 37, 1, (2012) DOI;10.1016/j.jhsa.2011.09.027
URL	http://hdl.handle.net/2241/115335

doi: 10.1016/j.jhsa.2011.09.027

1 **Correlation of histopathology with magnetic resonance imaging in Kienböck disease**

2
3 *Takeshi Ogawa M.D., Ph.D., **Yasumasa Nishiura M.D., Ph.D., **Yuki Hara M.D.,
4 Ph.D., ***Yoshikazu Okamoto M.D., Ph.D., **Naoyuki Ochiai M.D., Ph.D.

5
6 * Department of Orthopaedic Surgery, Kikkoman general hospital, 100 Miyazaki, Noda,
7 Chiba, 278-0005, Japan

8 **Department of Orthopaedic Surgery, Graduate School of Comprehensive Human
9 Sciences, University of Tsukuba, 1-1-1 Tennodai, Tsukuba, Ibaraki, 305-8575, Japan

10 *** Department of Radiology, Graduate School of Comprehensive Human Sciences,
11 University of Tsukuba, 1-1-1 Tennodai, Tsukuba, Ibaraki, 305-8575, Japan

12
13 *Corresponding author:* Takeshi Ogawa, M.D. Ph.D.

14 Department of Orthopaedic Surgery, Kikkoman general hospital, 100 Miyazaki,
15 Noda-shi, Chiba 278-0005, Japan

16 Tel: +81-4-7123-5911. Fax: +81-4-7123-5920.

17 E-mail address: oga-take@pg7.so-net.ne.jp

18 **【A running title】**

19 Correlation of histopathology with MRI in Kienböck disease

20 **【Key words】**

21 Kienböck disease, histopathology, magnetic resonance imaging, lunate, bone necrosis

22 **【Acknowledgement】**

23 The authors thank Masayuki Noguchi, M.D., Ph.D. (Department of Pathology, Institute
24 of Basic Medical Science, Graduate School of Comprehensive Human Science,
25 University of Tsukuba, Tsukuba, Ibaraki, Japan) for the technical assistance and good
26 advice for pathology.

27

28 **Introduction**

29 The treatment of Kienböck disease remains controversial; however, it is agreed that
30 early diagnosis is important.¹⁻³ Magnetic resonance imaging (MRI) of Kienböck disease
31 typically gives a uniformly low signal on T1-weighted images. MRI is essential for an
32 early diagnosis.^{4, 5} However, it is difficult to understand the detail of the actual histology,
33 which can enable the selection of appropriate treatment options. Few reports have
34 correlated MRI scans and histopathological appearances of biopsy specimens^{6, 7} or
35 comparisons with sagittal sections of whole lunate bones.⁸ As compared to the
36 histological findings, low-intensity areas on MRI did not correlate closely with the
37 extent of the necrotic areas and did not distinguish between new bone formation and
38 granulation tissue. Moreover, Hashizume et al. said that this disagreement was due to
39 the poor quality of the MRI.⁸ Schmitt et al. summarized the pathoanatomic processes
40 and the corresponding MRI findings in the natural course of lunate osteonecrosis.⁹ In
41 close correlation with the underlying pathoanatomic processes, 3 different signal and
42 contrast enhancement patterns can be identified in lunate osteonecrosis with the use of
43 contrast-enhanced, T1-weighted MRI. This imaging technique clearly shows the
44 different enhancement patterns and differentiation between bone marrow edema and
45 partial and complete bone marrow necrosis.^{9,10}

46 The purpose of this study was to compare in the detail pre-surgery MRI scans with the
47 corresponding coronal sections of extirpated lunates of patients with Kienböck disease.
48 Our hypothesis is that the MRI scans taken with 47-mm microscopy surface coil are
49 reflected the histopathology of Kienböck disease.

50 **Materials and methods**

51 Six patients (3 men and 3 women; aged 21–64 years; average 38 years) with Kienböck

52 disease underwent tendon-ball replacement¹¹ or the Graner surgical procedure (lunate
53 excision, capitate osteotomy, and intercarpal arthrodesis)^{12,13} between 2005 and 2008 at
54 our Hospital. Each patient was examined by radiography and MRI. Lichtman's criteria
55 were used to identify stage 3b Kienböck disease on the x-ray.

56 MRI was performed within 1 month before surgery using a 1.5-T system (Gyrosan NT
57 Intera; Phillips Medical Systems, Best, The Netherlands). Coronal 2-dimensional
58 proton-density weighted (PDW) (T1-weighted) (repetition time [TR][msec]/echo time
59 [TE][msec] = 1697-1852/17.0) images, and fast-field echo (FFE)(T2-weighted) (TR/TE
60 = 392-396/13.8-14.0) images of the wrist were acquired using a 47-mm microscopy
61 surface coil (Philips Medical Systems, Best, The Netherlands). The microscopy coil is
62 intended for a range of applications requiring a small field of view while maintaining a
63 high signal-to-noise ratio and is well suited to examine small anatomical lesions. The slice
64 thickness was 1.5-mm, and the slice interval was 0.1-mm with a field of view of
65 50-mm.^{14,15} Under these conditions, the lunate bones were imaged in 8 slices of the
66 coronal view. A radiologist (Y.O.) and the author (T.O.) observed all preparations and
67 evaluated the images.

68 The whole lunate bones were extirpated during replacement surgery and were fixed in
69 a 10% buffered neutral formalin solution (Wako®, Osaka, Japan). After decalcification
70 in 0.5 M EDTA, 0.1 M Tris and NaOH for 4 months, the samples were embedded in
71 paraffin. The decalcified whole lunates were sectioned roughly into 8 coronal specimens
72 (Fig. 1) correlating with the coronal MRI and were stained with hematoxylin-eosin.
73 Given that a long axis of the lunate was about 20mm, the width of 8 coronal specimens
74 was about 2mm. Since the slice thickness of MRI was 1.5mm, the error was presumed to
75 be up to about 1mm.

76 Assessment points of histopathological osteonecrosis included observations of empty
77 lacunae, fatty marrow, and vascular structures, and the findings were compared with
78 the signal levels of the PDW- and FFE-coronal MRI at the same slice levels. The author
79 (T.O.) and another researcher (Y.H.) familiar with histopathological evaluations made
80 the histological observations of the slices. In total, 8 views from the MRI and 8 slices of
81 the histopathological specimens that were similar in shape macroscopically were
82 compared by the author (T.O.) with regards to the assessment points of
83 histopathological osteonecrosis.

84

85 **Results**

86 Generally, PDW images of normal lunates exhibit high signal intensities, whereas FFE
87 images exhibit intermediate intensities.⁷ In comparison, the PDW images of the necrotic
88 lunate in this study demonstrated lower signal intensities, and the FFE images
89 exhibited higher or lower intensities.¹⁶ The overall MRI and histopathological
90 observations of each diseased lunate are shown in Table 1. Sagittal diagrams include
91 images taken from the central part of the coronal view (Fig. 2). Histopathological
92 analyses revealed disrupted trabecular and degraded fatty marrows towards the center
93 of the lunates. However, on the dorsal and palmar aspects of the lunates, the trabecular
94 structures, fatty marrows, and blood vessels appeared normal. Likewise, the palmar
95 and dorsal aspects of the lunates maintained near-normal intensities as observed in the
96 PDW images.

97 The pre-surgical MRI and histopathological images of a representative case are shown
98 Figure 3. Towards the center of the lunate, the signal intensity of the PDW images was
99 reduced, and segmented trabecular structures were observed in the corresponding

100 histopathological views. The details of a representative slice level are shown (Fig. 3c, k,
101 s). Within the solid outline (Fig. 4, upper row), the region appeared nearly normal
102 histopathologically because we could observe trabecular structures and fatty marrow
103 (Fig. 4a). This region also exhibited high intensity PDW images and moderate intensity
104 FFE images. Furthermore, the observed signal was equal to the signal of the normal
105 osseous tissue in the MRI. Conversely, within the dotted outline (Fig. 4, upper row), the
106 region was filled with fibrous granular tissue and blood vessels, and no fatty marrow or
107 osteocyte nuclei were observed histopathologically (Fig. 4b). This region also exhibited
108 slightly low intensity PDW images and high intensity FFE images. In all specimens, we
109 observed a signal change on the MRI, as well as changes in the histopathology. In the
110 dorsal distal region (Fig. 3a, i, q), near-normal signal intensities were observed on the
111 MRI, and normal trabecular structures were observed in the histopathological analyses,
112 including osteocyte nuclei, fatty marrow, and blood vessels. This region also exhibited
113 high intensity PDW images and intermediate intensity FFE images (Fig. 3a, i, q). In the
114 volar 1/3 area (Fig. 3f, n, v) of the lunate, there were fibrous granular tissues and blood
115 vessels but an absence of fatty marrow, and this area exhibited low intensity PDW
116 images and high intensity FFE images.

117 Of the 6 patients having Kienböck disease (stage 3b), osteocyte nuclei, fatty marrow,
118 and blood vessels were present within the corresponding high intensity areas of the
119 PDW images. In the low intensity areas of the PDWs, osteocyte nuclei and fatty marrow
120 were absent, and blood vessels were only present in some of the histopathological
121 findings. The intensities of the FFE images and the histopathological findings did not
122 always correlate (Table 2).

123

124 **Discussion**

125 In normal bone, T1-weighted MRI images have a high signal, and T2-weighted MRI
126 images show an intermediate signal. However, in the early stages of osteonecrosis,
127 T1-weighted images exhibit a low signal, and T2-weighted images show a high signal.
128 This intensity change reflects a loss of fatty marrow affecting the T1 signal and possible
129 edema contributing to a high signal in the T2-weighted images. In the more advanced
130 stages of osteonecrosis, T1- and T2-weighted images both show low signal intensities.¹⁶
131 In the present cases, the lunate conditions were assumed to be advanced osteonecrosis
132 because of stage 3b on x-ray; however, the MRI scans using a 47-mm microscopy coil
133 showed a variety of focal changes.

134 Desser et al. (1990) showed that MRI was able to distinguish areas of viable and
135 nonviable bone within the lunate. They further demonstrated that undecalcified,
136 fluorescently-labeled histological sections of lunate biopsies exhibited tetracycline
137 uptake.⁷ Trumble et al. (1990) showed that 6 patients having a diagnosis of Kienböck
138 disease demonstrated a correlation between the loss of signal intensity on T1- and
139 T2-weighted MRI images and evidence of osteonecrosis by histology. However, the
140 extent of marrow changes that must be present for signal intensity alterations in MRI
141 scans has not been determined.⁶ Hashizume et al. (1996) histologically examined
142 extracted whole lunates from 10 patients with Kienböck disease (stage 3). All of the
143 patients showed a markedly decreased intensity of the lunate on MRI in sagittal
144 T1-weighted images. In T2-weighted images, 2 cases showed complete low intensity,
145 and 3 cases yielded diffuse images that included mixed high and low areas. MRI (T1-
146 and T2-weighted images) low-intensity areas did not correlate closely with the extent of
147 the necrotic areas in the histological findings and did not distinguish between new bone

148 formation and granulation tissue in detail. Moreover, they said that this disagreement
149 was due to the poor quality of the MR images.⁸ In our 6 cases, empty lacunae and a
150 reduction of fatty marrow, but not the presence of blood vessels, correlated with the
151 signal intensities of the PDW images taken with a 47-mm microscopy coil.

152 Kienböck disease is denoted as an avascular necrosis because blood vessels are usually
153 not present. In the lunates of our study, the trabecular bone structures were segmented,
154 and fatty marrows were absent, which potentially allowed the formation of fibrous
155 granulation tissues, although with the presence of blood vessels. Hashizume et al.
156 (1996) reported that necrotic areas were invaded with new bone formation and
157 granulation. The necrotic tissue then changed into fibrous scar tissue and necrotic
158 debris. Around the necrotic area, non-necrotic tissues under hypervascularized
159 conditions were reactive to the necrosis.⁸ Even if there are blood vessels
160 histopathologically, it is unknown whether there is effective blood flow or interosseous
161 pressure when evaluated by MRI. If we can know the effective blood flow in the lunate,
162 it may be useful for selecting treatment or elucidating the etiology of Kienböck disease.

163 Schmitt et al. (2007) classified 3 patterns for Kienböck disease by using
164 contrast-enhanced MRI and described this classification as the best evaluation for the
165 viability of bone marrow.⁹ Certainly, to evaluate blood flow and the bone marrow edema
166 of the lunate in detail, gadolinium enhanced MRI is necessary.

167 The absence of gadolinium enhancement in our study is a limitation. Additional
168 limitations include the small number of cases, low field strength, and minimal imaging
169 conditions.

170

171 **References**

- 172 1. Beredjikian PK. Kienbock's disease. *J Hand Surg* 2009; 34A:167-175.
- 173 2. Innes L, Strauch RJ. Systematic review of the treatment of Kienbock's disease
174 in its early and late stages. *J Hand Surg Am* 2010; 35:713-7, 17 e1-4.
- 175 3. Squitieri L, Petruska E, Chung KC. Publication bias in Kienbock's disease:
176 systematic review. *J Hand Surg Am* 2010; 35:359-367 e5.
- 177 4. Amadio PC, Hanssen A D, Berquist TH. The genesis of Kienbock's disease:
178 evaluation of a case by magnetic resonance imaging. *J Hand Surg Am* 1987;
179 12:1044-1049.
- 180 5. Imaeda T, Nakamura R, Miura T, Makino N. Magnetic resonance imaging in
181 Kienbock's disease. *J Hand Surg Br* 1992; 17:12-19.
- 182 6. Trumble TE, Irving J. Histologic and magnetic resonance imaging correlations
183 in Kienbock's disease. *J Hand Surg Am* 1990; 15:879-884.
- 184 7. Desser TS, McCarthy S, Trumble T. Scaphoid fractures and Kienbock's disease
185 of the lunate: MR imaging with histopathologic correlation. *Magn Reson*
186 *Imaging* 1990; 8:357-361.
- 187 8. Hashizume H, Asahara H, Nishida K, Inoue H, Konishiike T. Histopathology of
188 Kienbock's disease. Correlation with magnetic resonance and other imaging
189 techniques. *J Hand Surg Br* 1996; 21:89-93.
- 190 9. Schmitt R, Krimmer H. Osteonecrosis of the hand skeleton. In: Schmitt R,
191 Lanz U, eds. *Diagnostic Imaging of the Hand*. 1st ed. Stuttgart, New
192 York: Georg Thieme Verlag; 2007; 351-364.
- 193 10. Schmitt R, Christopoulos G, Kalb K, Coblenz G, Frohner S, Brunner H,
194 Krimmer H, Lanz U. Differential diagnosis of the signal-compromised lunate in

195 MRI. *Rofo* 2005; 17: 358-366.

196 11. Ueba Y, Nosaka K, Seto Y, Ikeda N, Nakamura T. An operative procedure for
197 advanced Kienbock's disease. Excision of the lunate and subsequent
198 replacement with a tendon-ball implant. *J Orthop Sci* 1999; 4:207-215.

199 12. Graner O, Lopes EI, Carvalho BC, Atlas S. Arthrodesis of the carpal bones in
200 the treatment of Kienbock's disease, painful ununited fractures of the
201 navicular and lunate bones with avascular necrosis, and old
202 fracture-dislocations of carpal bones. *J Bone Joint Surg Am* 1966; 48: 767-774.

203 13. Takase K, Imakiire A. Lunate excision, capitate osteotomy, and intercarpal
204 arthrodesis for advanced Kienbock disease. Long-term follow-up. *J Bone Joint*
205 *Surg Am* 2001; 83: 177-183.

206 14. Tanaka T, Yoshioka H, Ueno T, Shindo M, Ochiai N. Comparison between
207 high-resolution MRI with a microscopy coil and arthroscopy in triangular
208 fibrocartilage complex injury. *J Hand Surg Am* 2006; 31: 1308-1314.

209 15. Yoshioka H, Ueno T, Tanaka T, Kujiraoka Y, Shindo M, Takahashi N, Nishiura
210 Y, Ochiai N, Saida Y. High-resolution MR imaging of the elbow using a
211 microscopy surface coil and a clinical 1.5 T MR machine: preliminary results.
212 *Skeletal Radiol* 2004; 33: 265-271.

213 16. Schmitt R, Heinze A, Fellner F, Obletter N, Struhn R, Bautz W. Imaging and
214 staging of avascular osteonecroses at the wrist and hand. *Eur J Radiol* 1997;
215 25: 92-103.

216

217 **Figure legends**

218 Figure 1. Whole lunate with a schema of the 8 coronal slices scanned using MRI.

219 Figure 2. MRI analysis of each patient. Sagittal diagrams include images taken from
220 the central part of the coronal view.

221 Figure 3. Pre-surgical PDW images (a–h) and FFE images (i–p) and HE stained sections
222 (q–x) (x 12.5) taken from the dorsal to palmar side of the lunate from a 21-year-old
223 left-handed woman that underwent a Graner surgical procedure for Kienböck disease
224 (stage 3b).

225 Figure 4. Representative slice levels (taken from Fig. 2c, k, s) and correlating histology.
226 Within the solid outline (upper row), the region appeared nearly normal
227 histopathologically because we could observe trabecular structures and fatty marrow (a).
228 This region also exhibited high intensity PDW images and moderate intensity FFE
229 images and was equal to the signal of the normal osseous tissue in the MRI. Conversely,
230 within the dotted outline (upper row), this region contained fibrous granular tissue and
231 blood vessels, and no fatty marrow or osteocyte nuclei were observed histopathologically
232 (b). (a) A high magnification image of the squared encircled area in (c, k and s).
233 Osteocyte nuclei, fatty marrow, and blood vessels are present within the vitalized focal
234 area of the solid line. (b) Fibrous granular tissues and blood vessels are present,
235 whereas there is an absence of fatty marrow within the dotted line.

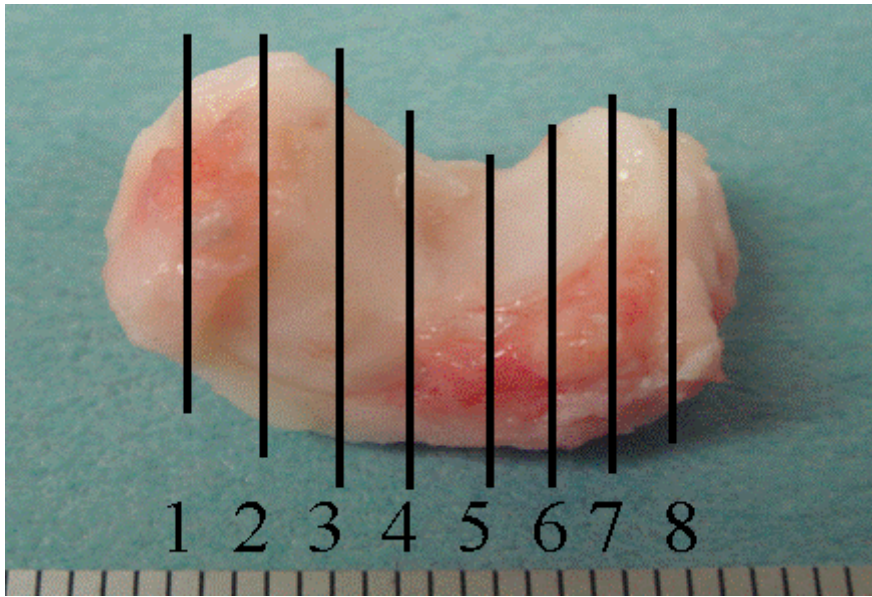
236

237 Table 1. MRI and histopathological analysis of each patient.

238 Table 2. Correlation of the histopathology with the MRI scans: (+), presence; (±),
239 discordance; (-), absence.

240

241 Figure 1.



242

243

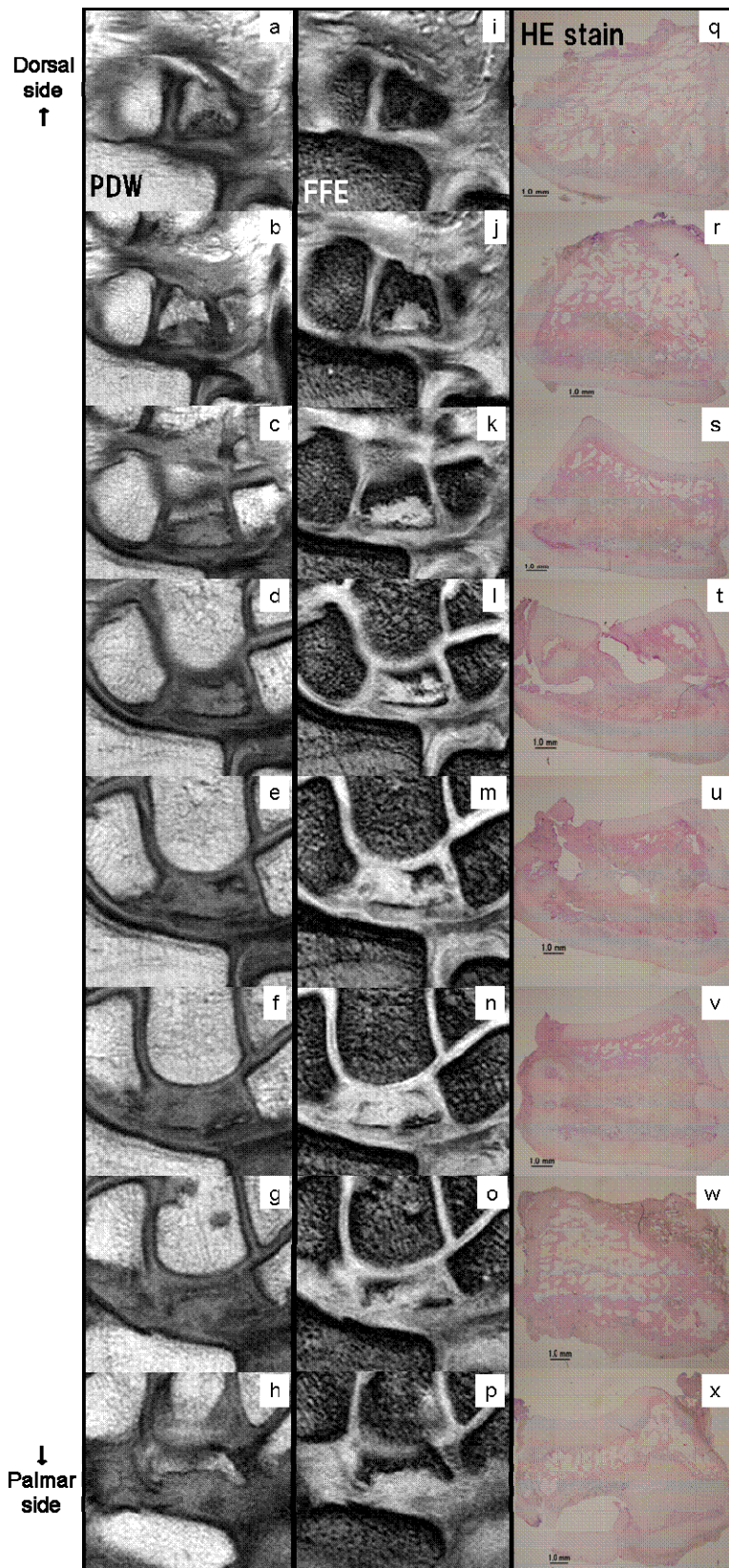
244 Figure 2.

245

246

Patient	MRI finding			
	PDW		FFE	
		sagittal diagram		sagittal diagram
1	normal or partial slightly low (dorsal 1/3 and volar 1/3), low (central 1/3)		normal (dorsal 1/3 and volar 1/4), low (another central part)	
2	normal (dorsal 1/2), low (volar 1/2)		normal (dorsal 1/2), low (volar 1/2)	
3	normal (dorsal 1/4 and volar-ulnar sides), low (dorsal 1/4 to volar-radial sides)		high (dorsal 1/3 and volar-ulnar sides), low (dorsal 1/3 to volar-radial sides)	
4	all slices are slightly low		all slices are high and low (diffuse or partial)	
5	low (volar 1/4), another slices are slightly low		normal (dorsal 1/3), high (diffuse or partial) (center to volar side)	
6	normal or partially slight low (dorsal 1/3 and volar 1/3), low (central 1/3)		high (dorsal 3/4), normal (volar 1/4)	
Normal	hyperintense signal		intermediate signal	

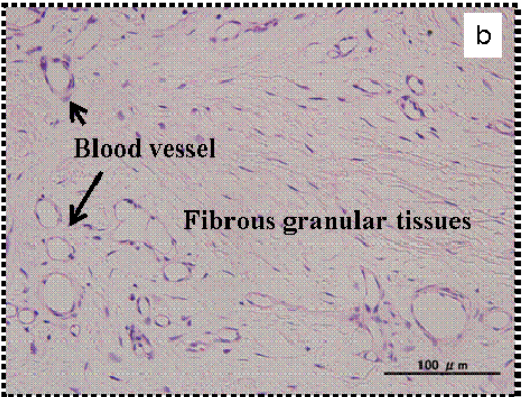
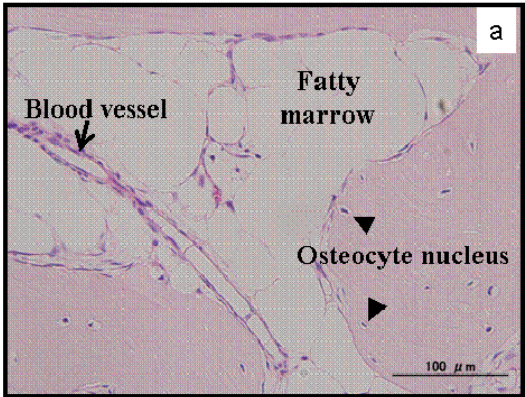
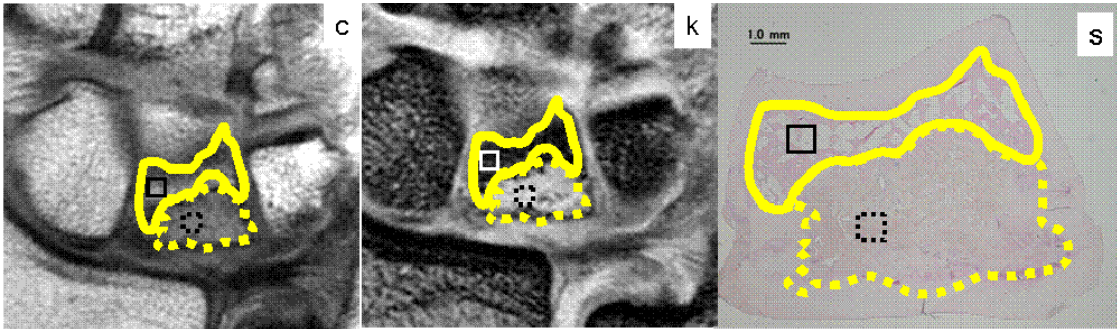
247 Figure 3.



248

249

250 Figure 4.



251

252

253 Table 1.

Patient	Gender	Age	X-ray finding	Histopathological finding			MRI finding	
				Empty lacunae	Fatty marrow	Blood vessel	PDW	FFE
1	F	65	segmentation and comminuted fracture at central 1/3	partially presence (central 1/3), a few (dorsal 1/3 and volar 1/3)	absence (central 1/3), partially presence (dorsal 1/3 and volar 1/3)	partially presence in all slices	normal or partial slightly low (dorsal 1/3 and volar 1/3), low (central 1/3)	normal (dorsal 1/3 and volar 1/4), low (another central part)
2	M	24	segmentation at volar 1/3	presence (dorsal1/3), absence (volar2/3)	presence (dorsal1/3), absence (volar2/3)	presence (dorsal1/3), absence (volar2/3)	normal (dorsal1/2), low (volar1/2)	normal (dorsal1/2), low (volar1/2)
3	M	21	severe collapse, especially radial side	partially presence in all slices	partial presence (dorsal1/4 and volar-ulnar side)	partially presence in all slices	normal (dorsal1/4 and volar-ulnar sides), low(dorsal 1/4 to volar-radial sides)	high (dorsal1/3 and volar-ulnar sides), low (dorsal 1/3 to volar-radial sides)
4	M	33	segmentation(+) coronal and sagittal plane on center	partially presence in all slices	partially presence (dorsal 1/3) , absence (central to volar 1/3)	partially presence in all slices	all slices are slightly low	all slices are high and low (diffuse or partial)
5	F	64	segmentation at volar 1/3	presence (dorsal2/3), absence (volar1/3)	absence in all slices	dorsal2/3 is absence, volar1/3 is presence	low (volar1/4), another slices are slightly low	normal (dorsal 1/3), high(diffuse or partial)(center to volar side)
6	F	21	segmentation and comminuted fracture at volar 1/3	partially presence (central 1/3), a few (dorsal 1/3 and volar 1/3)	absence (central 1/3), partially presence (dorsal 1/3 and volar 1/3)	partially presence in all slices	normal or partially slight low (dorsal 1/3 and volar 1/3), low (central 1/3)	high (dorsal3/4), normal (volar 1/4)
	Normal		sclerotic change (-) collapse (-) segmentation(+)	absence	presence	presence	hyperintense signal	intermediate signal

254

255

256 Table 2.

257

MRI finding		Histopathological finding			osteonecrosis
		Osteocyte nucleus	Fatty marrow	Blood vessel	
PDW image	intermediate	+	+	+	-
	slightly low	-	-	±	+
	low	-	-	±	+
FFE image	high	±	±	±	±
	intermediate	+	+	+	-
	low	±	±	±	±

258

259

260 **Abstract**

261 **Purpose** Diagnosis and treatment remain controversial for Kienböck disease. A few
262 reports have correlated magnetic resonance imaging (MRI), which is essential for early
263 diagnosis, and histopathology of Kienböck biopsy specimens, but histopathological
264 correlations of whole lunate bones or histological slices compared with MRI images are
265 lacking. The purpose of this study was to compare pre-surgical MRI scans taken with a
266 47-mm microscopy surface coil with corresponding histological slices of Kienböck
267 diseased lunates.

268 **Materials and methods** Extirpated whole lunates were harvested at the time of
269 surgery from 6 patients with Kienböck disease (stage 3b) undergoing tendon-ball
270 replacement or a Graner surgical procedure. Paraffin-embedded, coronally sectioned
271 specimens were stained with hematoxylin-eosin and compared with pre-surgical coronal
272 scans using MRI with a 47-mm microscopy surface coil.

273 **Results** Towards the center of the lunates, the signal intensity in the proton-density
274 weighted (PDW) images was reduced, whereas the dorsal and palmar sides of the
275 lunates exhibited no changes in intensity. In correlation, histopathological findings
276 revealed strongly disrupted trabeculae toward the center of the lunates and intact
277 trabeculae in the dorsal side of the lunates. Likewise, the necrotic and vitalized bone
278 exhibited low and high signal intensities, respectively, in the PDW images; however, in
279 the fast-field echo (FFE) images, there were no correlations with the histopathological
280 observations.

281 **Conclusions** MRI (PDW images, but not FFE images) using a 47-mm microscopy coil
282 reflected the extent and localization of the necrotic area in Kienböck diseased lunates,
283 as evidenced by comparison with histological analyses of the lunate specimens.